AEOLIAN FEATURES AS GROUND TRUTH FOR ATMOSPHERIC MODELING ON MARS. R. K. Hayward[1], L. K. Fenton[2], K. L. Tanaka[1], T. N. Titus[1], A. Colaprete[3], and P. R. Christensen[4], [1]U.S.G.S., 2255 N. Gemini Dr., Flagstaff, AZ 86001, rhayward@usgs.gov, [2]Carl Sagan Center/Ames Research Center, Moffett Field, CA, [3]NASA/Ames Research Center, Moffett Field, CA, [4]Arizona State University, Tempe, AZ.

Introduction: Sand dunes are among the most widespread aeolian features present on Mars, serving as unique indicators of the interaction between the atmosphere and surface. Both the presence and morphology of sand dunes are sensitive to subtle shifts in wind circulation patterns and strengths. Dunes are particularly suited to comprehensive planetary studies because they are abundant over a wide range of elevations and terrain types, are well exposed with distinct physical properties, and are well preserved, so that even inactive dunes yield information about the conditions under which they formed. Thus dunes provide a global-scale record of surface/atmosphere interaction. Here we consider four dune characteristics as possible records of "ground truth" and compare them to General Circulation Model (GCM) output. The four characteristics are: 1) geographic distribution, 2) dune type/morphology, 3) relative position within craters (dune centroid azimuth), and 4) slipface orientation. We compare these dune characteristics to the Ames Mars GCM, which is also part of the Mars Global Digital Dune Database (MGD[3]) [1].

Background: Aeolian dunes form where a source of sand exists, winds of saltation strength are available to carry sand downwind, and winds subsequently weaken below the threshold for sand transport [2]. Since Viking-era images revealed evidence of Martian dune fields three decades ago, researchers have been using the physical characteristics of those dunes, as well as other aeolian features, to predict local and global wind patterns, e.g. [3], [4], and [5]. The use of Geographic Information Systems (GIS), makes it possible to more effectively compare aeolian features to atmospheric models by using global databases. MGD[3] provides an important link between the global geographic distribution of dune fields and their local, physical characteristics.

Methods: MGD[3] was constructed using Thermal Emission Imaging System (THEMIS) infrared (IR) images [6] to locate and digitize potential dune fields from 90ºN to 90ºS. Those dune fields were divided into three regions. The equatorial region, displayed in green, Figure 1, was released in 2007 as United States Geological Survey (USGS) Open-File Report (OFR) 2007-1158 [7] (http://pubs.usgs.gov/of/2007/1158/). Preliminary data have been collected for regions poleward of 65°N and 65°S. The north polar region (65ºN to 90ºN), displayed in yellow, will be the next region released. The south polar region (65ºS to 90ºS), displayed in red, will be released last. Detailed instructions on how to use MGD[3] are available [8] at http://www.lpi.usra.edu/meetings/dunes2008/pdf/7013.

Geographic Distribution. The most basic characteristic of dune fields related to atmospheric activity, their geographic distribution, is available as a natural outgrowth of mapping the dune fields. An initial data set of THEMIS IR band 9 images covering orbits 816-9601 (02/2002 - 02/2004; L_s = 0.085º-358.531º), comprising more than 30,000 images planet-wide, was chosen as the basis for the construction of the database. This provided 75% daytime and 98% nighttime coverage of Mars. Dunes were more difficult to identify on nighttime images, so actual coverage may be closer to 75%. Because the initial locations of dune fields are based on THEMIS IR images (resolution 100 m/px), only moderate to large-size dune fields are included in the database, with the smallest dune field ~ 1 km^2 in area. We do not include bright, ripple-like bedforms. While the moderate to large dune fields are likely to constitute the largest compilation of sand on the planet, smaller amounts are likely to be found elsewhere via higher resolution data. The absence of mapped dune fields does not mean that such dune fields do not exist and is not intended to imply a lack of saltating sand in other areas.

Dune Type. Another fundamental indicator of wind direction is the type of dune that forms. It has been observed on Earth that different wind regimes produce different dune morphologies. Because the resolution of THEMIS IR images was usually too low for dune classification, dunes were classified using higher resolution THEMIS VIS (18m/px) [6], Mars Orbiter Camera narrow angle (MOC NA) (generally 1.5 to 5m/px) [9], or Mars Reconnaissance Orbiter (MRO) Context Camera (CTX) (6m/px) images [10], where available. We use McKee's 1979 terrestrial classification system [11] and currently include barchan, barchanoid, dome, linear, star, transverse, and (for bodies of sand with no discernable shape) sand sheet. "Unclassified" dunes either lack suitably detailed images or do not readily fit the Earth-based dune classification system, possibly because they have been influenced by environmental conditions unique to Mars. McKee found that (on Earth) barchans, barchanoid and transverse dunes form under a unidirectional wind regime, while barchans with elongated horns and linear dunes may form under a bidirectional wind regime. Star dunes indicate a multi-directional wind regime. Note that when multiple dune types occur within a dune field, we assign all the appropriate dune types to the dune field. Due to the

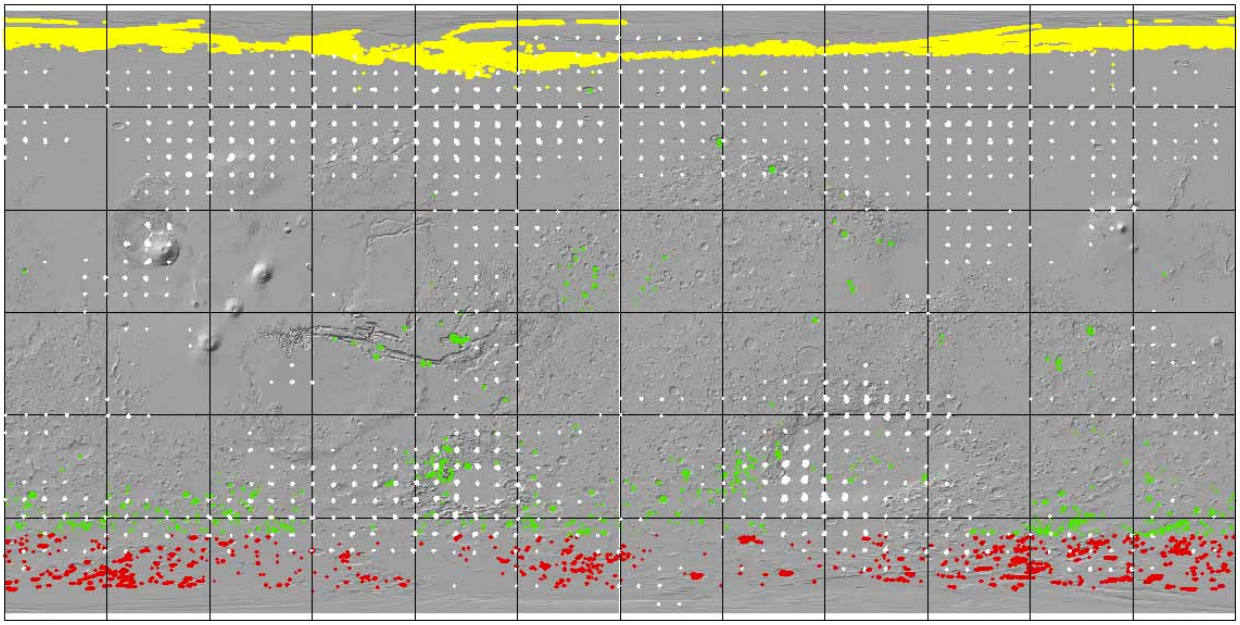

Figure 1. Global distribution of dune fields. Equatorial (released 2007) shown in green. North polar shown in yellow. South polar shown in red. GCM modeled winds with shear stress > .0225 N/m^2 threshold shown in white. Background is MOLA hillshade. Equidistant Cylindrical projection with 0°E center longitude.

global nature of the mapping, we do not specify the exact location of, or relative coverage by, each dune type.

Dune Centroid Azimuth. The first method we use to quantify wind direction is a measure of a dune field's relative location within a crater. Relative location within the crater might indicate the prevailing wind direction during the period of dune field migration across a crater floor. ESRI ArcMap® tools are used to locate the centroid (geographic center) of the crater, the centroid of the dune, and to calculate the azimuth of the line connecting the centroids. We refer to the resulting geodesic azimuth as the dune centroid azimuth.

In larger craters, central peaks, younger impacts or erosion may create topographic traps or obstructions within the crater. The resulting crater floor roughness may influence the location of a dune field more than wind direction. Dune centroid azimuth is most reliable as an indicator of wind direction when a single dune field occurs within a smooth-floored crater. More than 400 dune centroid azimuths have been calculated for the 65°N to 65°S region, with ~40 calculated for the 65°N to 90°N region.

Slipface Orientation. The second method we use to quantify wind direction is slipface orientation. The slipface vector begins on the upwind stoss slope and terminates on the lee slipface slope, indicating the direction of sediment transport and therefore the direction of prevailing winds during the latest period of major dune modification. Detailed study of slipfaces was beyond the scope of a global database, so we used only gross morphology of dunes formed by unidirectional winds (i.e. barchan, barchanoid and transverse dunes) to measure slipface orientation. For ease of plotting and comparison to the GCM, we averaged the individual (raw) slipface azimuths within each dune field. Slipface orientations are not meant to be used as evidence for current dune activity, nor to imply age constraints, as many of the identified dunes may be inactive. More than 10,000 raw slipface measurements are included in the 65°N to 65°S region, and more than 5,000 have been completed for the 65°N to 90°N region.

Modeled Wind Direction. Grid spacing for the Ames Mars GCM is based on 5 degrees of latitude by 6 degrees of longitude cells. Output was created for each Martian day in one Martian year. Shear stress, wind velocity and wind azimuth were provided 8 times daily. We use winds with a shear stress > .0225 N/m^2 for comparison to our directional data. Haberle et al. [12] have shown that setting a threshold stress of 0.0225 N/m^2 with the Ames Mars GCM will lift dust (through bombardment from sand saltation) in spatial patterns that qualitatively agree with observed dust storm occurrences. While we have chosen this threshold stress value, it is possible that sustained movement of sand may require long-term winds significantly above this threshold. For more details about the Ames Mars GCM see [13].

Discussion: *Geographic Distribution.* In a broad sense the geographic distribution of dune fields may be a record of atmospheric activity. If all other factors (e.g., source availability and topography) were equal, we would expect atmospheric circulation patterns to be reflected in dune field distribution, with dune fields occurring where winds were sufficiently strong to move sand grains. Therefore, as a first step we compare the global dune distribution pattern to GCM output. Dune fields do not uniformly cover Mars, but are concentrated from 35°S to 80°S and from 70°N to 83°N. Comparing the distribution to the GCM (Figure 1, global, GCM in white; Figure 2, north polar, GCM in yellow) shows that dune fields are frequently concentrated in areas where few modeled winds exceed the chosen threshold, while areas with more intense wind activity may have no dunes at all. The lack of GCM vectors in dune covered areas could be due to several factors: 1) the dunes may not have formed under the modeled wind regime, 2) the GCM's large grid size may have smoothed out small-scale wind gusts, 3) while winds of saltation strength are needed to initiate movement and keep sand moving, too many high winds may keep an area swept clean of sand, with dunes accumulating where winds are less intense, or 4) dune field distribution may be primarily constrained by other factors, such as availability of source materials. Comparison of dune distribution to mesoscale atmospheric model output may help address 1 and 2. Comparing dune models that start with point sources of sand to models that start with a blanket source may help assess the importance of number 4.

Dune Type. Dunes in the equatorial and north polar dune fields have strikingly similar morphologies, despite the differences in depositional environment (about 85% of equatorial dune fields were deposited in craters, compared to about 1% of north polar dune fields). Both regions are dominated by barchan, barchanoid and transverse (unidirectional) dunes. This supports earlier observations based on Viking images that reported unidirectional winds to be the dominant dune-forming wind regime on Mars [14].

Linear dunes and barchans with elongated horns, generally believed to form under a more complex wind regime, are not common in the equatorial region. When present, their lack of correlation to GCM modeled winds suggests that local winds, influenced by crater topography, may play a role in shaping them. Linear dunes in the north polar region, while still a minority, appear to be more abundant than in the equatorial region. Dune fields containing linear dunes (outlined in green, Figure 2), are concentrated between 0°E - 120°E and 300°E - 360°E and extend to a lower latitude than dune fields without linear dunes. In the north polar region the GCM modeled winds become more multi-directional with distance from the pole, which may explain, in part, the increased abundance of linear dunes. Alternatively, a longitudinal variation in wind regime complexity may be responsible.

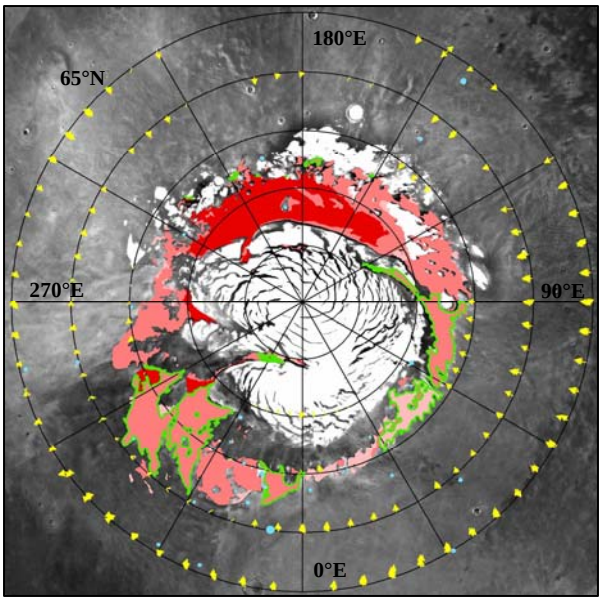

Figure 2. North polar dune field distribution. Red, closely spaced dunes. Dark pink, moderately spaced dunes. Light pink, widely spaced dunes [15]. Blue, craters with dune fields. Green outline, dune fields with some linear dunes. White, residual ice cap. Yellow, GCM >.0225N/m^2. Background is Viking MDIM.

Dune Centroid Azimuth. There are about 340 intracrater dune fields in the equatorial region, whose dune centroid azimuths were calculated and compared to the GCM. The comparison suggested that agreement varies with diameter of crater, with smaller craters (<25 km diameter) displaying better agreement (~65%). We hypothesize that this is because smaller diameter craters tend to have smoother floors, allowing unimpeded dune migration, and thus exhibit better correlation between their location and GCM modeled winds. In the north polar region we have only documented about 40 craters containing dune fields. Nearly all are less than 25 km in diameter. For about 70% of these the dune centroid azimuth agrees fairly well with the GCM modeled wind direction.

Slipface Orientation. When comparing slipfaces to GCM winds in the equatorial region, we found that agreement was not as good (~40%) as that of dune centroid azimuth and GCM winds, possibly because the nearby crater walls may affect local winds, and therefore dune morphology. A logical test of this would be to look at intercrater dunes. They are scarce in the equatorial region, but do show a somewhat bet-

ter correlation (50%) to the GCM output. In the north polar region, for intracrater dunes, the slipface to GCM agreement rate is only about 40%. For dunes in the circumpolar erg, agreement is very good in some areas, especially in the southern part of the erg (70°N to 75°N) between 250°E and 340°E. A notable exception occurs when slipface evidence suggests that winds locally funnel down chasmata. The GCM does not reflect this, perhaps due to its relatively coarse grid.

Examples with greater complexity. A combination of dunes and other aeolian features, such as wind streaks, can show evidence of varying wind direction on different time scales. In Figure 3, barchans indicate dune-forming winds from the SW, wind streaks indicate opposing winds from the ENE, but the GCM modeled winds (>.0225 N/m^2) indicate winds from the SSW. Areas with a more complex record may be especially useful as ground truth.

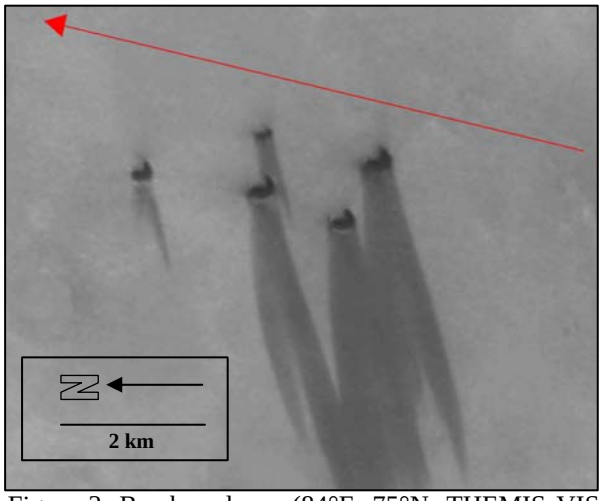

Figure 3. Barchan dunes (84°E, 75°N, THEMIS VIS image V11943005) indicate winds from SW. Wind streaks suggest winds from ENE. Red arrow represents GCM modeled wind direction (from SSW).

Summary: Four possible records of atmospheric behavior are presented here; geographic distribution of dune fields, dune type/morphology, dune centroid azimuth, and slipface orientation. The **geographic distribution** of dune fields may be a broad-brush indicator of long term regional atmospheric trends. Concentrations of dune fields are highest north of 70ºN and south of about 35ºS, which indicates that in these areas a) a sand source was available, b) atmospheric activity was great enough to allow sand transport, and c) where dune fields are now located, atmospheric activity dropped enough to cause the sand load to be deposited. **Dune type/morphology** suggests that the majority of dune fields planet-wide formed under the influence of unidirectional winds (resulting in barchan, barchanoid, and transverse morphologies). Linear dunes, thought to be produced when a secondary wind is present, are rarer, but are more common in the north polar region than the equatorial. Topographically influenced local winds, not resolved by a GCM, may play a role, especially for intracrater dunes. However, linear dunes may also indicate areas with more complex regional winds. **Dune centroid azimuth,** when calculated for dunes in smooth-floored craters, agrees moderately well with GCM modeled winds. It may be a fairly reliable record of broad regional atmospheric activity for the southern hemisphere, where intracrater dunes dominate. Agreement between **slipface orientation** and GCM output in intracrater dune fields is not as strong as between dune centroid azimuth and GCM output, suggesting that crater topography may influence local winds that control slipface development. Where local topography is less important (e.g. parts of the north polar erg) slipface orientation may more closely reflect the regional wind regime. The four records of atmospheric behavior discussed above are part of MGD^3, which is publicly available for the equatorial region (65ºN to 65ºS). Data for the north polar region (65ºN to 90ºN) and south polar region (65ºS to 90ºS) will soon be released.

Future work: Comparison of the records discussed above to strategically located (geographically and temporally) mesoscale models would help assess the value of dunes as ground truth. In addition, expansion of the database to include a broader scope of aeolian features that form on different time scales (e.g., transverse aeolian ridges, yardangs, ventifacts, wind streaks and dust devil tracks) would make the database a more powerful tool for atmospheric modelers.

Acknowledgements: This project was partially supported as part of the Mars Odyssey Thermal Emission Imaging Spectrometer Project (Arizona State University).

References: [1] Hayward R.K., et al. (2007) JGR, 112, E11007, doi 10.1029/2007JE002943. [2] Bagnold, R.A. (1941), London: Methuen, 265 pp. (reprinted 1954; 1960; 2005, Dover, Mineola, NY). [3] Ward, A.W. (1979) JGR, 84, 8147-8166. [4] Greeley, R. (1993) JGR, 98, 3183-3196. [5] Fenton, L.K. and M.I. Richardson (2001) JGR, 106, 32,885-32,902. [6] Christensen, P.R., et al., THEMIS Public Data Releases, PDS node, ASU, http://themis-data.asu.edu. [7] Hayward R.K., et al. (2007) U.S.G.S. Open File Rep., 2007–1158. [8] Hayward, R.K., et al. (2008), Planetary Dunes Workshop, 04/29-05/02, 2008, Alamogordo, NM, LPI Cont. No. 1403, 42-43. [9] Malin, M.C., et. al., Malin Space Science Systems Mars Orbiter Camera Image Gallery http://www.msss.com. [10] Malin, M.C. et al. (2007) JGR, 112, E055S04. [11] McKee, E.D. (1979). In: E.D. McKee (Editor), USGS Professional Paper 1052. [12] Haberle, R.M., et. al. (2003) Icarus, 161, 66-89. [13] Haberle, R.M., et. al. (1999) JGR, 104, 8957-8974. [14] Greeley, R., et.al. (1992) in *Mars*, ed. by H. Kieffer, et.al., 730-766, U. of Arizona Press, Tucson. [15] Tanaka, K.L and R.K. Hayward (2008), Planetary Dunes Workshop, 04/29-05/02, 2008, Alamogordo, NM, LPI Cont. No. 1403, 69-70.